

Polymorphism of monolayer lipid membrane structures made from unsymmetrical bolaamphiphiles

Mitsutoshi Masuda,^{a,b,*} Kenji Yoza^c and Toshimi Shimizu^{a,b}

^aNanoarchitectonics Research Center (NARC), National Institute of Advanced Industrial Science and Technology (AIST), Tsukuba Central 5, 1-1-1 Higashi, Tsukuba, Ibaraki 305-8565, Japan

^bCREST, Japan Science and Technology Agency (JST), Tsukuba Central 4, 1-1-1 Higashi, Tsukuba, Ibaraki 305-8562, Japan

^cBruker AXS Co. Ltd, 309-A, Moriya, Kanagawa, Yokohama, Kanagawa 221-0022, Japan

Received 25 April 2005; accepted 18 August 2005

Available online 5 October 2005

Abstract—The crystal structures of synthetic unsymmetrical 1-glucosamide- and 1-galactosamide bolaamphiphiles, 13-[(β-D-glucopyranosyl)carbamoyl]tridecanoic acid (**1**) and 15-[(β-D-galactopyranosyl)carbamoyl]pentadecanoic acid (**2**), respectively, were elucidated by single-crystal X-ray analysis. The space group for **1** is $P2_1$, $Z = 2$ with cell dimensions: $a = 8.6816(9)$, $b = 4.8578(5)$, $c = 26.250(3)$ Å, $\beta = 91.460(2)^\circ$; that for **2** $P2_1$, $Z = 2$ with cell dimensions: $a = 4.90(1)$, $b = 40.139(1)$, $6.289(1)$ Å, $\beta = 106.48(1)^\circ$. The glucopyranosyl and galactopyranosyl rings in **1** and **2**, respectively, take a 4C_1 chair conformation. In the crystal lattice, the 1-glucosamide **1** forms a symmetrical monolayer lipid membrane (MLM) structure in which the molecules are packed in an antiparallel fashion, while 1-galactosamide **2** has an unsymmetrical MLM with parallel molecular packing. The stereochemistry of the sugar hydroxy group proved to affect their hydrogen-bonding networks and induce the polymorphism of the MLM.
© 2005 Elsevier Ltd. All rights reserved.

Keywords: X-ray; Single-crystal X-ray structures; Unsymmetrical bolaamphiphile; Monolayer lipid membrane; Hydrogen-bond network; Polymorphism

1. Introduction

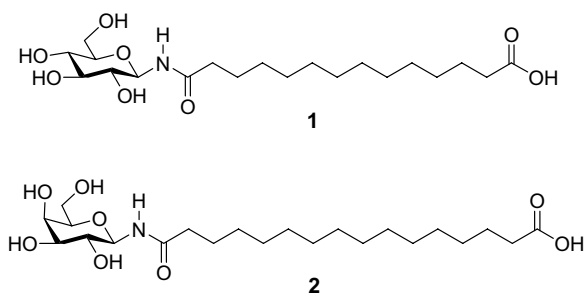
Heteroditopic 1,ω-bipolar amphiphiles, so-called ‘unsymmetrical bolaamphiphiles’, in which two headgroups that differ in size or properties are linked to a hydrophobic spacer at each end, are one of the cell-membrane components of thermophilic and acidophilic *archaeobacteria*.^{1,2} These have been known to form highly stable monolayer lipid membranes (MLMs).^{3,4} The MLMs are classified into an unsymmetrical and a symmetrical type, depending on whether their component amphiphiles are packed in a parallel or antiparallel fashion within the MLMs, that is to say ‘polymorphism’.^{3,5} Several attempts have aimed to control the polymorphism of bolaamphiphiles because the molecular packing affects not only the self-assembled mor-

phologies like solid fibers^{6–10} and tubes,^{5,10–13} but also their dimensions from nanometers to micrometers.¹³ In addition, the vesicles or tubes consisting of the unsymmetrical MLMs can differentiate their internal and external surfaces.¹⁴ Therefore, efficient and selective filling of nanomaterials into their hollow nanospace can be expected.¹⁵

We have previously reported the self-assembly behavior of the unsymmetrical bolaamphiphile **1** and the longer chain homologues of **1**, which have a 1-glucosamide headgroup at one end of an oligomethylene chain and a carboxylic acid at the other. They self-assembled in water to form nanotubes and microtubes simultaneously, depending on the polymorphism of the MLMs.¹³ The nanotubes made from **1** transformed into single crystals by acidification. Herein, we describe details of the crystal structure of **1** together with 1-galactosamide analogue **2**.¹⁶ The molecular structures, packings, subcell types and hydrogen-bonding (H-bonding)

* Corresponding author. Fax: +81 298 61 4545; e-mail: m-masuda@aist.go.jp

networks of **1** and **2** are discussed in terms of the polymorphism. Our results suggest that the stereochemistry of the sugar hydroxy groups, in either an axial or an equatorial position, affects the H-bonding network, the presence or absence of clathrated water, and polymorphism. To the best of our knowledge, this is the first example of polymorphism in an MLM structure that depends on the stereochemistry of sugar headgroups of the unsymmetrical bolaamphiphiles.



2. Experimental

The syntheses of 13-[(β -D-glucopyranosyl)carbamoyl]tridecanoic acid (**1**) and 15-[(β -D-galactopyranosyl)carbamoyl]pentadecanoic acid (**2**) have been reported elsewhere.¹³ The single crystal of **1** was prepared by acidification of an aqueous dispersion (pH < 4) of self-assembled nanotubes of **1** (1.0 mg/mL) by vapor diffusion of acetic acid,¹³ while that of **2** was obtained upon cooling from a hot MeOH solution (6.1 mg/mL). The crystallization of **1** from MeOH solution gave a colorless powder, and the aqueous solution of **2** yielded thin fibrous solids. The data collections of X-ray diffraction peaks for **1** and **2** were carried out on a Bruker M06XHF22/SMART APEX automatic CCD diffractometer and a Rigaku AFC7R automatic four-circle diffractometer, respectively. Crystal data and summary of the experimental details are given in Table 1. The structures were solved by direct methods (SHELEX-97¹⁷) and expanded using Fourier techniques. The absolute configurations of the molecules were determined by the known chirality of the D-glucose- and D-galactose rings for **1** and **2**, respectively, in previous syntheses.^{18,19} All non-hydrogen atoms were refined anisotropically. The hydrogen atoms of O–H and N–H were located by differential Fourier synthesis, and the bond lengths of O–H and N–H were normalized to 0.97 and 1.03 Å, respectively. The remaining hydrogen atoms were placed at calculated position [$d(\text{C–H}) = 0.99$ Å]. The atomic coordinates of the non-hydrogen and hydrogen atoms attached to oxygen and nitrogen for **1** and **2** are listed in Table 2. The bond distances and angles, selected torsion angles, and CIF files are attached as Supplementary data.

Table 1. Crystal data and summary of experimental details for **1** and **2**

Bolaamphiphile	1	2
Empirical formula	C ₂₀ H ₃₇ N ₁ O ₈ ·H ₂ O	C ₂₂ H ₄₁ N ₁ O ₈
Formula weight	437.53	447.57
Temperature (K)	90	302
Wavelength (Å)	0.71073 (Mo K α)	1.54178 (Cu K α)
Crystal system	Monoclinic	Monoclinic
Space group	<i>P</i> ₂ ₁	<i>P</i> ₂ ₁
Unit cell dimensions		
<i>a</i> (Å)	8.6816(9)	4.90(1)
<i>b</i> (Å)	4.8578(5)	40.139(1)
<i>c</i> (Å)	26.250(3)	6.289(1)
β (°)	91.460(2)	106.48(1)
Volume (Å ³)	1106.7(2)	1187.3(3)
<i>Z</i>	2	2
Calculated density (g/cm ³)	1.313	1.260
Absorption coefficient (mm ⁻¹)	0.102	0.0779
Crystal size (mm)	0.53 × 0.24 × 0.02	0.20 × 0.20 × 0.1
θ range for data collection (°)	0.782–27.87	0.6–119
Index ranges	–8 ≤ <i>h</i> ≤ 11 –6 ≤ <i>k</i> ≤ 6 –34 ≤ <i>l</i> ≤ 34	0 ≤ <i>h</i> ≤ 5 0 ≤ <i>k</i> ≤ 45 –7 ≤ <i>l</i> ≤ 7
Reflections collected	7504	2038
Independent reflections	4835	1936
Absorption correction	Empirical	Psi-scan
Goodness-of-fit on <i>F</i> ²	1.174	1.27
<i>R</i> factor	0.065	0.031
<i>wR</i> (<i>F</i> ²)	0.156	0.096

3. Results and discussion

3.1. Molecular structure

The molecular structures and packing of **1** and **2** in the crystal lattices are shown in Figures 1 and 2, respectively. The pyranose rings of both bolaamphiphiles take the ⁴C₁ conformation, and the hydrophobic spacer all-*trans* conformation (Fig. 1). 1-Glucosamide bolaamphiphile **1** forms a monohydrated crystal, while 1-galactosamide **2** forms an anhydrous crystal. The C–C bond lengths are normal, 1.492(4)–1.539(4) and 1.492(3)–1.531(3) Å for **1** and **2**, respectively, as are the C–O, 1.400(3)–1.416(3) and 1.405(3)–1.441(2) Å for **1** and **2**, respectively (see Supplementary data). All bond angles and torsion angles show normal values.

Table 3 summarizes the Cremer–Pople puckering parameters (*Q*, θ and ϕ)²⁰ of the pyranose rings in **1** and **2**, together with values of the ideal rings.²¹ In general, the parameter *Q* indicates a total deviation of the ring atoms from mean plane of the pyranose ring, while the θ and ϕ indicate a relative orientation of their puckering, that is, chair, boat, skew, half-chair, and envelope conformations.²⁰ The smaller *Q* value of **1** than that of the ideal ring suggests that the chair conformations of the ring in **1** become slightly more planar than the ideal glucopyranosyl ring. The θ and ϕ values of the pyranose ring of **1** are, however, close to the ideal value of the

Table 2. Atomic coordinates and equivalent isotropic temperature factor^{a,b} for **1** and **2**

Molecule	Atom	<i>x/a</i>	<i>y/b</i>	<i>z/c</i>	<i>U</i> _{iso}
1	C(1)	−0.2914(3)	0.3833(6)	0.34270(11)	0.0118(6)
	C(2)	−0.1776(3)	0.5400(7)	0.37805(11)	0.0119(6)
	C(3)	−0.2277(3)	0.5183(6)	0.43245(11)	0.0107(6)
	C(4)	−0.3944(3)	0.6004(6)	0.43644(11)	0.0095(6)
	C(5)	−0.4955(3)	0.4405(6)	0.39914(11)	0.0105(6)
	C(6)	−0.6606(3)	0.5298(7)	0.39916(11)	0.0133(6)
	C(7)	−0.2338(4)	0.2268(6)	0.25749(12)	0.0168(7)
	C(8)	−0.2083(4)	0.3243(7)	0.20430(11)	0.0175(6)
	C(9)	−0.0777(4)	0.1762(7)	0.17890(11)	0.0145(6)
	C(10)	−0.0504(4)	0.2918(7)	0.12625(11)	0.0160(6)
	C(11)	0.0832(3)	0.1629(7)	0.09955(11)	0.0144(6)
	C(12)	0.1101(4)	0.2885(7)	0.04778(11)	0.0149(6)
	C(13)	0.2461(3)	0.1652(7)	0.02066(11)	0.0135(6)
	C(14)	0.2728(3)	0.2939(7)	−0.03078(11)	0.0142(6)
	C(15)	0.4086(3)	0.1727(7)	−0.05779(11)	0.0142(6)
	C(16)	0.4362(4)	0.2935(7)	−0.10987(11)	0.0161(6)
	C(17)	0.5710(4)	0.1646(7)	−0.13576(12)	0.0173(7)
	C(18)	0.5972(4)	0.2692(7)	−0.18948(12)	0.0175(7)
	C(19)	0.7388(4)	0.1342(8)	−0.21158(13)	0.0217(7)
	C(20)	0.7670(4)	0.1863(8)	−0.26655(12)	0.0170(6)
	N(1)	−0.2559(3)	0.4284(6)	0.29132(10)	0.0135(5)
	O(2)	−0.0289(2)	0.4314(5)	0.37441(9)	0.0189(5)
	O(3)	−0.1329(3)	0.6953(5)	0.46238(9)	0.0173(5)
	O(4)	−0.4415(2)	0.5487(5)	0.48681(8)	0.0129(5)
	O(5)	−0.4422(2)	0.4821(4)	0.34920(8)	0.0113(4)
	O(6)	−0.6723(2)	0.8135(5)	0.38756(8)	0.0128(4)
	O(7)	−0.2357(4)	−0.0149(5)	0.26833(10)	0.0299(6)
	O(8)	0.8690(3)	0.0670(6)	−0.28825(9)	0.0281(6)
	O(9)	0.6751(3)	0.3646(5)	−0.28797(9)	0.0213(5)
	O(W)	0.9055(2)	0.5378(5)	0.56166(8)	0.0122(4)
	H(N-1)	−0.258(4)	0.569(10)	0.2827(14)	0.016
	H(O-2)	0.006(4)	0.489(8)	0.3462(14)	0.016
	H(O-3)	−0.139(4)	0.671(9)	0.4948(15)	0.016
	H(O-4)	−0.471(5)	0.679(9)	0.4964(15)	0.016
	H(O-6)	−0.751(5)	0.856(8)	0.4033(14)	0.016
	H(O-9)	0.680(4)	0.386(8)	−0.3200(15)	0.016
H(1w)	0.942(4)	0.688(5)	0.5788(12)	0.016	
H(2w)	0.983(3)	0.415(6)	0.5581(13)	0.016	
2	C(1)	0.3505(3)	0.56529(5)	−1.2185(3)	0.0296(4)
	C(2)	0.1447(4)	0.56589(5)	−1.4507(3)	0.0314(4)
	C(3)	0.1916(3)	0.59745(5)	−1.5699(3)	0.0319(4)
	C(4)	0.1753(4)	0.62818(5)	−1.4331(3)	0.0340(4)
	C(5)	0.3733(4)	0.62429(5)	−1.1976(3)	0.0332(4)
	C(6)	0.3443(5)	0.65337(5)	−1.0533(3)	0.0430(5)
	C(7)	0.5282(3)	0.51709(5)	−0.9855(3)	0.0318(4)
	C(8)	0.4495(4)	0.48655(5)	−0.8731(3)	0.0363(4)
	C(9)	0.6591(4)	0.47941(5)	−0.6486(3)	0.0397(5)
	C(10)	0.5783(5)	0.44882(6)	−0.5375(3)	0.0446(5)
	C(11)	0.7919(4)	0.44092(6)	−0.3173(3)	0.0437(5)
	C(12)	0.7170(5)	0.40979(6)	−0.2049(4)	0.0467(5)
	C(13)	0.9289(5)	0.40152(6)	0.0158(4)	0.0470(5)
	C(14)	0.8539(5)	0.37049(6)	0.1260(4)	0.0484(5)
	C(15)	1.0664(5)	0.36230(6)	0.3475(4)	0.0488(5)
	C(16)	0.9914(5)	0.33125(7)	0.4568(4)	0.0498(5)
	C(17)	1.2039(5)	0.32291(6)	0.6772(4)	0.0518(6)
	C(18)	1.1274(5)	0.29194(6)	0.7878(4)	0.0505(6)
	C(19)	1.3405(5)	0.28335(6)	1.0072(4)	0.0538(6)
	C(20)	1.2584(5)	0.25294(6)	1.1185(4)	0.0526(6)
	C(21)	1.4633(5)	0.24514(7)	1.3413(4)	0.0549(6)
	C(22)	1.3791(5)	0.21582(6)	1.4542(4)	0.0494(5)
	N(1)	0.3122(3)	0.53649(4)	−1.0950(2)	0.0332(3)
O(2)	0.2004(3)	0.53717(4)	−1.5622(2)	0.0435(3)	
O(3)	−0.0143(3)	0.59983(4)	−1.7805(2)	0.0420(3)	

Table 2 (continued)

Molecule	Atom	x/a	y/b	z/c	U_{iso}
	O(4)	−0.1122(3)	0.63190(4)	−1.4298(2)	0.0444(4)
	O(5)	0.3056(2)	0.59418(4)	−1.0986(2)	0.0334(3)
	O(6)	0.5647(5)	0.65608(5)	−0.8548(3)	0.0739(5)
	O(7)	0.7768(3)	0.5228 ^c	−0.9790(2)	0.0444(3)
	O(8)	1.1826(6)	0.19853(6)	1.3692(4)	0.1017(7)
	O(9)	1.5421(5)	0.21005(6)	1.6517(3)	0.0838(6)
	H(N-1)	0.106(2)	0.5289(6)	−1.105(4)	0.054(6)
	H(O-2)	0.053(4)	0.5382(7)	−1.702(3)	0.065(7)
	H(O-3)	0.089(5)	0.5978(8)	−1.890(4)	0.074(8)
	H(O-4)	−0.122(7)	0.6560(2)	−1.421(5)	0.078(9)
	H(O-6)	0.660(7)	0.6354(5)	−0.801(6)	0.09(1)
	H(O-9)	1.506(7)	0.1890(4)	1.714(5)	0.075(9)

^a The expression $U_{\text{iso}} = 1/3 \sum \sum U_{ij} a_i^* a_j^* \cdot a_j^*$.

^b Standard deviations are given in parentheses.

^c Fixed parameter.

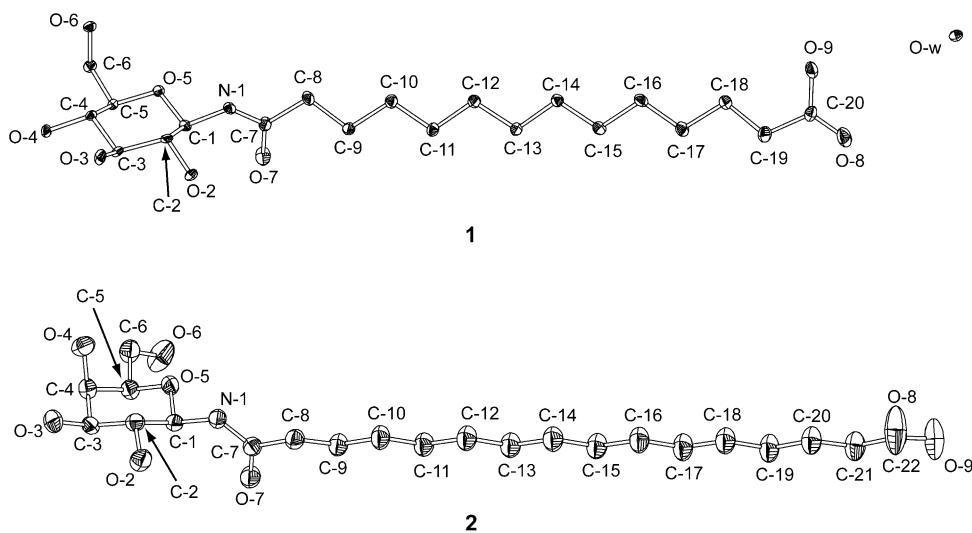


Figure 1. Molecular structures (ORTEP drawing) and atomic numbering for **1** and **2**. Thermal ellipsoids are drawn at 50% probability.

ring. In contrast, the slightly larger θ value of **2** than that of the ideal ring and the ϕ value of 23.8° indicate that the chair conformation of **2** is slightly deformed to a half-chair.²¹

3.2. Molecular packing

Figure 2 shows both bolaamphiphiles **1** and **2** self-assembled into MLM structures. The 1-glucosamide bolaamphiphile **1** packed into an antiparallel motif is categorized into a symmetrical MLM, while the galactosamide analogue **2** goes into a parallel motif, an unsymmetrical MLM. The clathrated water of **1** is located between the pyranose rings packed in a side-by-side fashion, which enlarges the repeating distance of the rings from 6.289 \AA (c -axis of **2**) to 8.6816 \AA (a -axis of **1**, see Table 1 and Fig. 2). As a result, the cross-sectional area of the pyranose headgroup also increases from

29.6 \AA^2 in **2** to 42.2 \AA^2 in **1** (Table 4). The enlarged packing of the pyranose headgroup in **1** accommodates the smaller carboxylic acid group of **1** between them. Thus, the clathrated water stabilizes pseudo interdigitation of the carboxylic group in the symmetrical MLM structure.

3.3. Subcell packing

The observed polymorphism in the MLM of **1** and **2** is also clear from the spacer chain packing, namely the 'subcell structure'.²² The subcell structure of **1** in the symmetrical MLM is categorized as an O_\perp type, while that of **2** is a T_\parallel type, as shown in Table 4. The 2-fold screw axis of the $P2_1$ space group exists along the b -axis in the crystal lattice of **1**. In addition, the zigzag chain plane of the spacer is non-parallel to the 2-fold screw axis. Therefore, the chains should pack alternately into

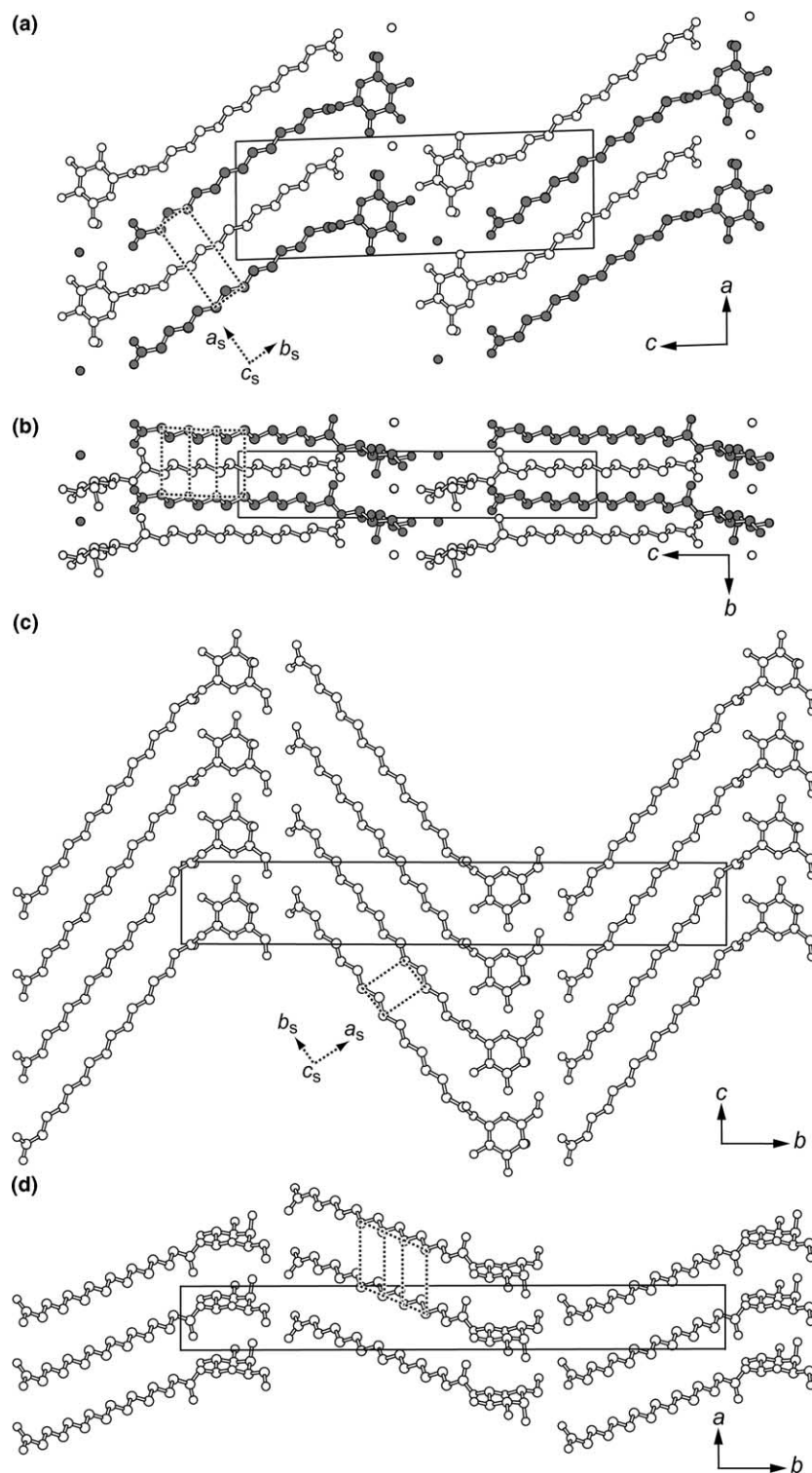


Figure 2. Molecular packing of **1** viewed along (a) the b -axis and (b) the a -axis and that of **2** viewed along (c) the a -axis and (d) the c -axis. Hydrogen atoms are omitted for clarity. Dotted lines and arrows with a_s , b_s , and c_s indicate the subcells and their axes.

non-parallel arrangement, such as the O_{\perp} type, by the symmetry operation. In contrast, the 2-fold screw axis locates along the c -axis in the crystal **2**, and the zigzag chain plain packs in the same direction to form the T_{\parallel} type.

3.4. The MLM thickness and molecular length

The MLM thickness (d) of the unsymmetrical type estimated from the cell parameter of **2** is shorter than the extended molecular length (L) of **2**.¹³ In contrast, that

Table 3. Cremer–Pople puckering parameters²⁰ for the pyranose ring of **1** and **2** in crystal

Molecule	Q	θ (°)	ϕ (°)
1	0.566	3.7	352.2
2	0.585	4.9	23.8
Glucose ^a	0.598	3.7	358.0
Galactose ^b	0.586	3.7	21.5

Ideal values for energy minimized ^a β -D-glucopyranose and ^b β -D-galactopyranose.²¹

of the symmetrical type is wider than the L of **1**, even if the spacer chain is tilted by 35° with respect to normal to the layer plane (Table 4). This is because the bolaamphiphile **1** in the symmetrical MLM seems to offset each other to widen the d -value. This structure resembles the interdigitated bilayer structure of 1-decyl α -D-glucopyranoside,²³ if one regards the carboxylic acid group of

1 as a methyl end terminal. In the unsymmetrical MLM of **2**, the spacer chain is deeply tilted by 52° to trade off the difference of the cross-sectional areas between the galactopyranose ring and the spacer methylene chains (29.6 Å² and 18.3 Å², respectively, as shown in Table 4).

3.5. H-bonding scheme

H-bonding networks of the sugar hydroxy and amide groups are shown in Figure 3, and their dimensions are summarized in Table 5. The sugar hydroxy, amide, and carboxylic acid groups form multiple H-bonding networks and stabilize the MLM stacking structures in both **1** and **2** crystals. However, the differences in the stereochemistries of the sugar headgroups alter the H-bonding scheme and induce the polymorphism of the MLMs as mentioned above. The intralayer H-bonding

Table 4. Summary of the molecular packings and the packing parameters of **1** and **2** in the crystal lattice

	Molecule	
	1	2
MLM type	Symmetrical	Unsymmetrical
Molecular packing	Antiparallel	Parallel
Idealized subcell type and its dimensions	O_{\perp} $a_s = 7.07, b_s = 2.52, c_s = 4.86$ Å	T_{\parallel} $a_s = 4.21, b_s = 2.54, c_s = 4.91$ Å $\alpha = 88.4^{\circ}, \beta = 62.5^{\circ}, \gamma = 84.9^{\circ}$
Cross-sectional area of headgroup ^a	42.2 Å ²	29.6 Å ²
Cross-sectional area of chain ^b	17.2 Å ²	18.3 Å ²
Tilt angle of chains	35°	52°
Molecular length (L) ^c and MLM thickness (d) ^d	L (2.52 nm) < d (2.62 nm)	L (2.77 nm) > d (2.01 nm)

^a Estimated from ab and ac plane of unit cell in **1** and **2**, respectively.

^b Estimated from the subcell dimensions.

^c Estimated from molecular modeling.

^d Estimated from the cell parameters of the crystal of **1** and **2**.

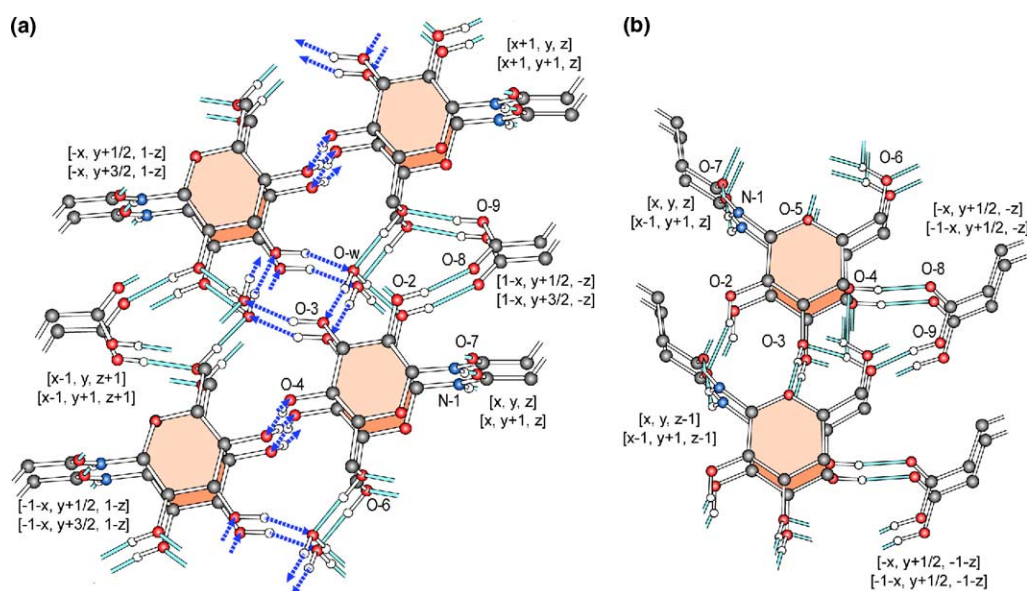
**Figure 3.** Three-dimensional hydrogen-bonding networks formed between sugars and carboxylic acids of (a) **1** and (b) **2**, viewed along the b and a directions, respectively. The finite and infinite chains of hydrogen bonds are shown in light blue lines and dotted blue arrows, respectively.

Table 5. Hydrogen-bond distances (Å) and angles (°) of **1** and **2** with symmetry codes

D–H	A	H···A (Å) ^a	D···A (Å)	D–H···A (°) ^a	Sym. code of A
1					
O(2)–H	O(8)	1.81	2.76	166	1 – x, y + 1/2, –z
O(3)–H	O(w) ^b	1.78	2.73	169	x – 1, y, z + 1
O(4)–H	O(4) ^b	1.77	2.73	170	–1 – x, y + 1/2, 1 – z
O(6)–H	O(w)	1.73	2.68	168	2 – x, y + 1/2, –z
O(9)–H	O(6)	1.81	2.63	161	–2 – x, y – 1/2, 2 – z
O(w)–H	O(2)	1.85	2.75	167	–x – 1, y + 1/2, 2 – z
O(w)–H	O(3)	1.78	2.67	169	–x – 1, y – 1/2, 2 – z
N(1)–H	O(7)	1.75	2.77	172	x, y + 1, z
2					
O(2)–H	O(7)	1.98	2.90	159	x – 1, y, z – 1
O(3)–H	O(5)	1.91	2.88	178	x, y, z – 1
O(4)–H	O(8) ^b	1.78	2.74	169	–x; 1, y + 1/2, –z
O(6)–H	O(3) ^c	2.12	3.01	152	x + 1, y, z + 1
O(6)–H	O(4) ^c	2.29	2.86	117	x + 1, y, z + 1
O(9)–H	O(6) ^b	1.68	2.88	171	x, y – 1/2, z + 2
N(1)–H	O(7)	2.01	2.97	153	x – 1, y, z

^a The H···A distances and D–H···A angles were calculated by normalizing the covalent O–H and N–H distance to the standard values of 0.97 and 1.03 Å, respectively.

^b Interlayer hydrogen bond.

^c Three-centered hydrogen bonds.

scheme in **2** is more similar to the symmetrical 1-glucosamide bolaamphiphile²⁴ than that in **1**. The intralayer H-bonding scheme of **2** exhibits 'N'-type H-bonds, O(4)···H–O(6)···O(3)···O(5), and double-accepter type of amide H-bonds, O(2)–H···O(7)···H–N(1). In contrast, **1** forms a three-dimensional H-bond network including two types of infinite chains, such as a zigzag motif of $\cdots[\text{O}(4)\text{--H}]_{\infty}\cdots$ and symmetry-related helical motif of $\cdots[\text{O}(3)\text{--H}\cdots\text{O}(w)\text{--H}]_{\infty}\cdots$ at the interface. Thus, the infinite chains are energetically more favorable than the finite chain²⁵ and contribute to stabilize the stacking of the unsymmetrical MLMs.

The carboxylic and sugar hydroxy groups in **1** form *intralayer* H-bond arrays consisting of O(8)···H–O(2) and O(9)–H···O(6), while those in **2** *interlayer* form arrays of O(8)···H–O(4) and O(9)–H···O(6). The differences between the inter- or interlayer hydrogen bonding obviously affect the polymorphism, such as the unsymmetrical or symmetrical MLM. In the symmetrical MLM of **1**, the carboxylic acid group somewhat retracts from the MLM interface and forms intralayer H-bonds because of the side-by-side packing of the 1-glucosamide headgroup. In contrast, the unsymmetrical MLM of **2** has two different interfaces covered with sugar and carboxylic acid headgroups. Thus, two different types of stacking motif of the MLM will be possible, such as a sugar–sugar interface or a sugar–carboxylic acid interface. In general, carboxylic acids tend to form a cyclic dimer with bifurcated H-bonds.²⁶ However, **2** forms H-bonds between the sugar hydroxy groups and the carboxylic acid, which have been so far been reported in a few examples such as carbohydrate-binding proteins.²⁷

Amide groups in both crystals form linear hydrogen bonds to enhance the stacking of pyranose ring. In the crystal of **2**, the amide oxygen atom O(7) also accepts a hydrogen of the O(2) hydroxy group as similarly observed in a crystal of 1-aldosamide bolaamphiphiles.^{24,28}

Supplementary data

Supplementary data of bond distances, bond angles, and selected torsion angles can be found, in the online version, at [doi:10.1016/j.carres.2005.08.005](https://doi.org/10.1016/j.carres.2005.08.005). A link via a footnote on the first page to the Supplementary data is provided in ScienceDirect. CCDC269751 and CCDC166281 contain the supplementary crystallographic data of **1** and **2**, respectively, for this paper. These data may be obtained free of charge via www.ccdc.cam.ac.uk/conts/retrieving.html (or from the CCDC, 12 Union Road, Cambridge CB2 1EZ, UK; fax +44 1223 336033, e-mail deposit@ccdc.cam.ac.uk).

References

1. Gliozzi, R. M.; Rolandi, R.; de Rosa, M.; Gambacorta, A. *J. Membr. Biol.* **1983**, *75*, 45–59.
2. Gulik, A.; Luzzati, V.; de Rosa, M.; Gambacorta, A. *J. Mol. Biol.* **1985**, *182*, 131–149.
3. Fuhrhop, J.-H.; Wang, T. *Chem. Rev.* **2004**, *104*, 2901–2937.
4. Fuhrhop, J.-H.; Fritsch, D. *Acc. Chem. Res.* **1986**, *19*, 130–137.
5. Shimizu, T.; Masuda, M.; Minamikawa, H. *Chem. Rev.* **2005**, *105*, 1401–1443.
6. Jaeger, D. A.; Li, G.; Subotkowski, W.; Carron, K. T. *Langmuir* **1997**, *13*, 5563–5569.

7. Schneider, J.; Messerschmidt, C.; Schulz, A.; Gnade, M.; Schade, B.; Luger, P.; Bombicz, P.; Hubert, V.; Fuhrhop, J.-H. *Langmuir* **2000**, *16*, 8575–8584.
8. Zhou, S.; Xu, C.; Wang, J.; Gao, W.; Akhverdiyeva, R.; Shah, V.; Gross, R. *Langmuir* **2004**, *20*, 7926–7932.
9. Song, J.; Cheng, Q.; Kopta, S.; Stevens, R. C. *J. Am. Chem. Soc.* **2001**, *123*, 3205–3213.
10. Sirieix, J.; Lauth-de Viguerie, N.; Rivière, M.; Lattes, A. *New J. Chem.* **2000**, *24*, 1043–1048.
11. Claussen, R. C.; Rabatic, B. M.; Stupp, S. I. *J. Am. Chem. Soc.* **2003**, *125*, 12680–12681.
12. Fuhrhop, J.-H.; Helfrich, W. *Chem. Rev.* **1993**, *93*, 1565–1582.
13. Masuda, M.; Shimizu, T. *Langmuir* **2004**, *20*, 5969–5977.
14. Fuhrhop, J.-H.; David, H. H.; Mathieu, J.; Liman, U.; Winter, H. J.; Boekema, E. *J. Am. Chem. Soc.* **1986**, *108*, 1785–1791.
15. Fuhrhop, J.-H.; Tank, H. *Chem. Phys. Lipids* **1987**, *43*, 193–213.
16. Masuda, M.; Shimizu, T. *Chem. Commun. (Cambridge)* **2001**, 2422–2443.
17. Sheldrick, G. M. SHELEX97, University of Göttingen, 1997.
18. Micheel, F.; Klemer, A. *Adv. Carbohydr. Chem. Biochem.* **1961**, *16*, 85–97.
19. Garg, G.; Jeanloz, R. W. *Adv. Carbohydr. Chem. Biochem.* **1985**, *43*, 135–149.
20. Cremer, D.; Pople, J. A. *J. Am. Chem. Soc.* **1975**, *97*, 1354–1358.
21. Dowd, M. K.; French, A. D.; Reilly, P. J. *Carbohydr. Res.* **1994**, *264*, 1–19.
22. Garti, N.; Sato, K. *Crystallization and Polymorphism of Fats and Fatty Acids*; Marcel Dekker: New York, USA, 1988.
23. Moews, P. C.; Knox, J. R. *J. Am. Chem. Soc.* **1976**, *98*, 6628–6633.
24. Masuda, M.; Shimizu, T. *Carbohydr. Res.* **1997**, *302*, 139–147.
25. Jeffrey, G. A.; Saenger, W. *Hydrogen Bonding in Biological Structure*; Springer: Berlin, Germany, 1991.
26. Fuhrhop, J.-H.; Köing, J. *Membranes and Molecular Assemblies: The Synekinetic Approach*, 1st ed.; The Royal Society of Chemistry: Cambridge, UK, 1994.
27. Quioco, F. A. *Pure Appl. Chem.* **1989**, *61*, 1293–1306.
28. Masuda, M.; Shimizu, T. *Carbohydr. Res.* **2000**, *326*, 56–66.